

Comparative assessment of fiber SPR sensor for sensitivity enhancement using BaTiO₃ layer

N. MUDGAL^{*,1}, K. K. CHOURE¹, A. SAHARIA², A. AGARWAL³, M. K. FALASWAL¹, S. SAHU⁴, S. V. SINGH⁵, G. SINGH¹

¹Department of ECE, Malaviya National Institute of Technology, Jaipur, India

²Manipal University, Jaipur, India

³Swami Keshvanand Institute of Technology, Management & Gramothan, Jaipur, India

⁴Jabalpur Engineering College, Jabalpur, India

⁵Jaypee Institute of Information Technology, Noida, India

In this work, we have numerically simulated a fiber surface plasmon resonance sensor. This work explored a comparative assessment of three different metal layers (silver (Ag)/gold (Au)/copper (Cu)) over the unclad optical fiber. These layers are further protected with the barium titanate (BaTiO₃) layer. The results of the proposed structure are shown with the transmission spectra for the various refractive indexes and the performance of this structure with three different configurations (Ag+BaTiO₃, Au+BaTiO₃, and Cu+BaTiO₃) is investigated. After a comparative analysis, we found the highest sensitivity with the Au+BaTiO₃ configuration. Hence, the proposed structure can be suitable for biosensing applications.

(Received October 22, 2021; accepted April 7, 2022)

Keywords: Barium titanate, Sensitivity, Surface plasmon resonance, Fiber

1. Introduction

Surface plasmon resonance (SPR) is one of the prominent approaches which have its potential sensing applications in various fields including environmental science, biomedical etc. [1-3]. In this approach, a p-polarized or transverse magnetic (TM) polarized light excites the surface plasmons (SPs) at the metal-dielectric interface. This SPR mechanism was first best described by Kretschmann in 1968 in which a high refractive index (RI) prism is employed to couple light at the metal-dielectric interface surrounded by a sensing medium and angular interrogation technique is used to observe the sharp dip in the reflectivity spectrum at the resonance [4, 5]. The prism-based SPR sensors are widely used in many applications including biosensing and molecule detection [6, 7]. However, advantages including low cost, remote sensing, and miniaturization attract the attention of researchers in sensing applications for the SPR sensors based on fiber over the prism. For fiber SPR sensing, a glass prism is replaced with a fiber core, and a metal layer is deposited over unclad fiber. The sample to be detected is positioned around the layer of metal and the resonance wavelength shift with the RI change is observed for the investigation of the sensor performance [8-10]. Generally, gold, silver, and copper are used as plasmonic active metals. These are deposited over the surface of the unclad fiber core. The optical properties including complex refractive index, interband contributions, free electron contributions, frequency dependent dielectric constant, plasma effects, damping, and so on make these materials

ideal for SPR sensing applications [11, 12]. Gold is highly stable as compared to these materials. Silver and copper suffer from poor chemical stability and oxidize easily. This makes the SPR sensor less stable. Hence, a protective layer over the surface of these layers is a choice to make an SPR sensor more stable to improve the performance of these sensors [13-16]. The SPR technology in the fiber-based sensor was first introduced by Lidberg et al. in 1983 and this initiated the SPR sensor in the field of biosensing applications [17]. For more than a decade, these SPR sensors widely used in food safety, biomedical, environmental protection and biomolecule detection, etc. [18-22]. The biomolecule concentration is generally small for biomolecule detection, and the sample to be tested also contains other molecules. Hence, a sensor with high resolution, specificity and sensitivity is needed. Therefore, the sensitivity enhancement of the SPR sensor will play a major role in disease diagnosis and the biomedical field. Currently, research for the SPR sensor is focused on sensitivity enhancement by optimizing the sensor structure or by coating a different material over the surface of one metal film [23, 24].

Lately, various materials such as graphene, black phosphorus, and transparent oxides, etc. are seen in the research due to their enhanced plasmonics characteristics [25-28]. To improve sensing performance, it is necessary to use functional materials in the SPR systems. Recently, BaTiO₃ with low dielectric loss and high dielectric constant is seen in research [29-32]. In this study, we have designed a fiber SPR sensor with a protective layer of BaTiO₃ layer over a metal layer to enhance its sensitivity.

Here, three different configurations of a metal layer over BaTiO₃ are studied and compared with their transmission

spectra and sensitivities.

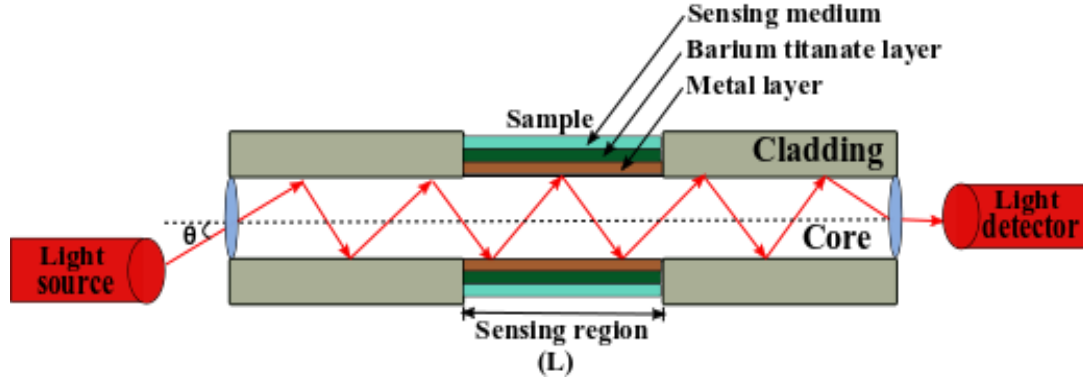


Fig. 1. Theoretical set-up of the proposed fiber-based SPR sensor (color online)

2. Structure modeling and theoretical formulation

Our proposed structure based on the attenuated total reflection technique of the Kretschmann arrangement is illustrated in Fig. 1. Here, a fiber core of fused silica is used to guide light waves from one side to the other side of the fiber, where a 20 mm length of fiber cladding is removed from the fiber. The diameter of the fiber silica core is 600 μm and the RI of fused silica core (n_{core}) can be given with the following dispersion relation [33],

$$n_{\text{core}}(\lambda) = \left(1 + \frac{a_1 \lambda^2}{\lambda^2 - b_1^2} + \frac{a_2 \lambda^2}{\lambda^2 - b_2^2} + \frac{a_3 \lambda^2}{\lambda^2 - b_3^2} \right)^{1/2} \quad (1)$$

Here, wavelength ' λ ' is in nm and the value of Sellmeier coefficients are: $a_1 = 0.6961663$, $b_1 = 0.0684043$, $a_2 = 0.4079426$, $b_2 = 0.1162414$, $a_3 = 0.8974794$, and $b_3 = 9.896161$.

Next, a metal layer is deposited over the unclad fiber. Here, we have taken a different metal layer of Ag, Au, and Cu for three different configurations. The thickness of all three layers is 40 nm and the dielectric constant of the metal layer (ϵ_{metal}) is calculated using following Drude model relation [34],

$$\epsilon_{\text{metal}}(\lambda) = 1 - \frac{\lambda^2 \lambda_c}{\lambda_p^2 (\lambda_c + i\lambda)} \quad (2)$$

Here λ_c represents collision wavelength and λ_p represents plasma wavelength. The values of λ_c and λ_p are as follow: for Ag metal layer, $\lambda_c = 1.7614 \times 10^{-5}$, and $\lambda_p = 1.4541 \times 10^{-7}$; for Au metal layer, $\lambda_c = 89.342 \times 10^{-7}$ and $\lambda_p = 1.6826 \times 10^{-7}$; for Cu metal layer, $\lambda_c = 4.0852 \times 10^{-5}$ and $\lambda_p = 1.3617 \times 10^{-7}$.

Further, the BaTiO₃ layer of a thickness of 10 nm is coated on the metal surface [20]. The dielectric constant of this BaTiO₃ layer is given as follows [35],

$$\epsilon_{\text{BaTiO}_3}(\lambda) = 1 + \frac{4.187 \lambda^2}{\lambda^2 - 0.223^2} \quad (3)$$

Finally, we have selected water as the sensing medium with the RI of 1.33 and observed the change in RI from 1.33 to 1.37 with a step change of 0.01 due to the biological reaction.

When the p-polarized light is launched into one side of the fiber, it travels to the other end and is completely reflected in the sensing area. Here the evanescent wave is generated that can excite the SPs at the metal-dielectric interface. For resonance, the wave vector of surface plasmon (β_{sp}) and incident light (k_x) should be equal. Mathematically [36],

$$k_x = \beta_{\text{sp}} \quad (4)$$

$$\frac{2\pi}{\lambda} n_{\text{core}} \sin \theta = \left\{ \frac{2\pi}{\lambda} \text{Re} \sqrt{\frac{\epsilon_m \epsilon_{\text{die}}}{\epsilon_m + \epsilon_{\text{die}}}} \right\} \quad (5)$$

where ϵ_m and ϵ_{die} denote the dielectric constant of metal and sensing medium respectively, n_{core} denotes the RI of the fiber core and λ denotes the incident light wavelength.

For p-polarized light incident at angle θ into the one end, the normalized transmitted power (P_{trans}) at the other end of the fiber can be written as follows [37],

$$P_{\text{trans}} = \frac{\int_{\theta_{\text{cr}}}^{\pi/2} R_p^{N_{\text{ref}}(\theta)} (n_1^2 \sin \theta \cos \theta / (1 - n_1^2 \cos^2 \theta)^2) d\theta}{\int_{\theta_{\text{cr}}}^{\pi/2} (n_1^2 \sin \theta \cos \theta / (1 - n_1^2 \cos^2 \theta)^2) d\theta} \quad (6)$$

where $N_{\text{ref}} = L/D \tan \theta$ represents the total number of reflections in the sensing area performed by a light ray, D and L represent the diameter of the fiber core and the

length of the sensing region respectively, $\theta_{cr} = \sin^{-1} n_{cl}/n_{core}$ represents the critical angle for the core-cladding interface while n_{cl} and n_{core} denote the RI of the cladding and core of the fiber respectively.

Reflectance (R_p) of this multilayer structure (core/metal/BaTiO₃/sensing medium) is calculated by Fresnel multilayer reflection theory and is given by [38],

$$R_p = r_p r_p^* = |r_p|^2 \quad (7)$$

Whereas the reflection coefficient (r_p) for p-polarized light is as follows,

$$r_p = \frac{q_1(M_{11}+M_{12}q_N)-(M_{21}+M_{22}q_N)}{q_1(M_{11}+M_{12}q_N)+(M_{21}+M_{22}q_N)} \quad (8)$$

Here, for the j^{th} layer, $M_j = \begin{bmatrix} \cos\beta_j & \frac{-i}{q_j} \sin\beta_j \\ -iq_j \sin\beta_j & \cos\beta_j \end{bmatrix}$ is

the characteristic matrix, in which transverse RI

$q_j = \sqrt{\left(\frac{1}{\epsilon_j}\right) \cos\theta_j} = \sqrt{(\epsilon_j - n_1^2 \sin^2\theta_1)}/\epsilon_j$ and phase factor $\beta_j = \left(\frac{2\pi}{\lambda}\right) n_j \cos\theta_j (z_j - z_{j-1})$; where $(z_j - z_{j-1})$ is the thickness of j^{th} layer.

The current sensor's output is focused on the sensitivity that is stated in respect of resonance wavelength change ($\delta\lambda$) and RI change (δn) in the sensing medium. Mathematically [39].

Sensor sensitivity,

$$(S_\lambda) = \frac{\delta\lambda}{\delta n} (nm/RIU) \quad (9)$$

The performance of the proposed sensor structure has been analysed using MATLAB simulation tool.

3. Results and discussions

We have numerically simulated the proposed setup of four layers structure given in Fig. 1. Here, the transfer matrix method (TMM) and Fresnel multilayer reflection theory are used to calculate the amplitude reflection coefficient at the multiple interfaces of this designed structure.

In this work, we have considered three different metal layers with the barium titanate layer for different RI ranging from 1.33 to 1.37. First, the Ag layer is considered and the transmission spectra for this configuration are illustrated in Fig. 2 (a-b) for RI 1.33, 1.34, 1.35, 1.36, and 1.37 of the sensing medium. In this, the normalized transmitted power with varying wavelengths can be calculated from the amplitude reflection coefficient by Eq. 6. Fig. 2 (a) depicts the normalized transmitted power spectra for the Ag layer without the BaTiO₃ layer. In this

figure, resonance wavelength (λ_{res}) is obtained at 471.1 nm for the RI of 1.33.

This changes to 653.4 nm with the Ag+BaTiO₃ configuration as illustrated in Fig. 2(b). The resonance wavelengths without the BaTiO₃ layer are obtained at 491.5 nm, 516.2 nm, 545.1 nm, and 579.7 nm for RI of 1.34, 1.35, 1.36, and 1.37 respectively. Similarly, the resonance wavelength for the Ag+BaTiO₃ configuration is obtained at 679.7 nm, 710.5 nm, 746.9 nm, and 791.1 nm for the RI of 1.34, 1.35, 1.36, and 1.37 respectively. Fig. 3 depicts the resonance wavelength variation with various RI for the Ag-based fiber SPR sensor with and without the BaTiO₃ layer.

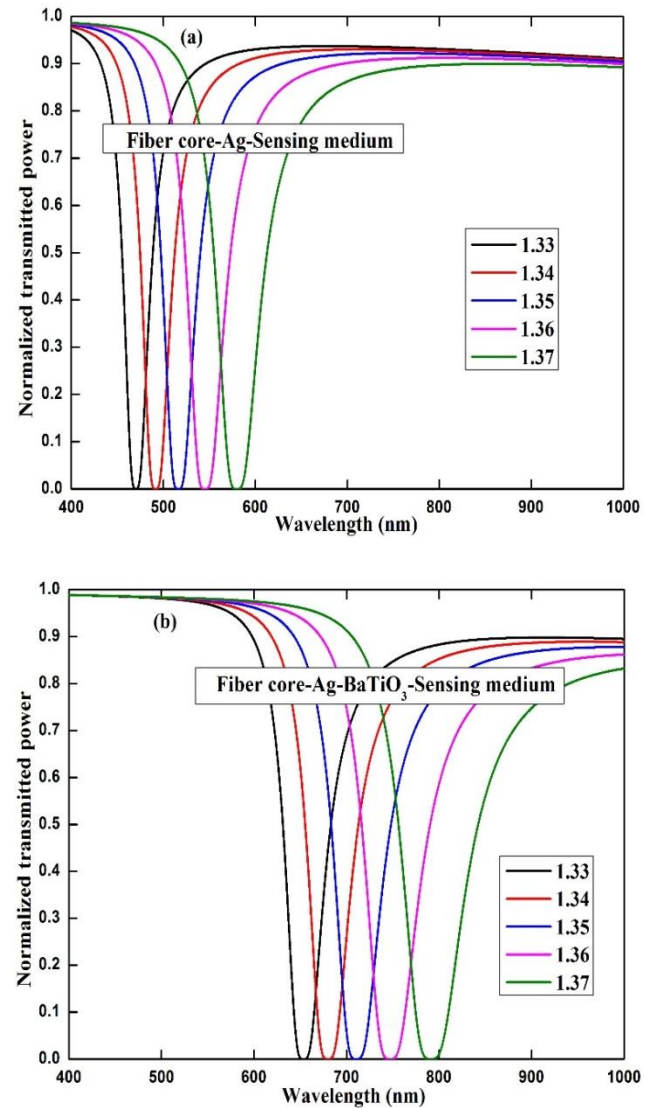


Fig. 2. Transmission spectra plot of Ag-based fiber SPR sensor (a) without BaTiO₃ layer (b) with BaTiO₃ layer (color online)

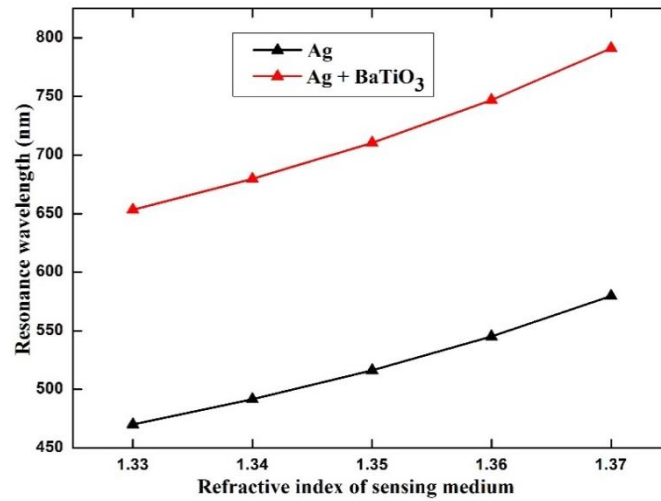


Fig. 3. Plot of resonance wavelength (nm) variation with various refractive indexes for Ag-based fiber SPR sensor with and without BaTiO₃ layer (color online)

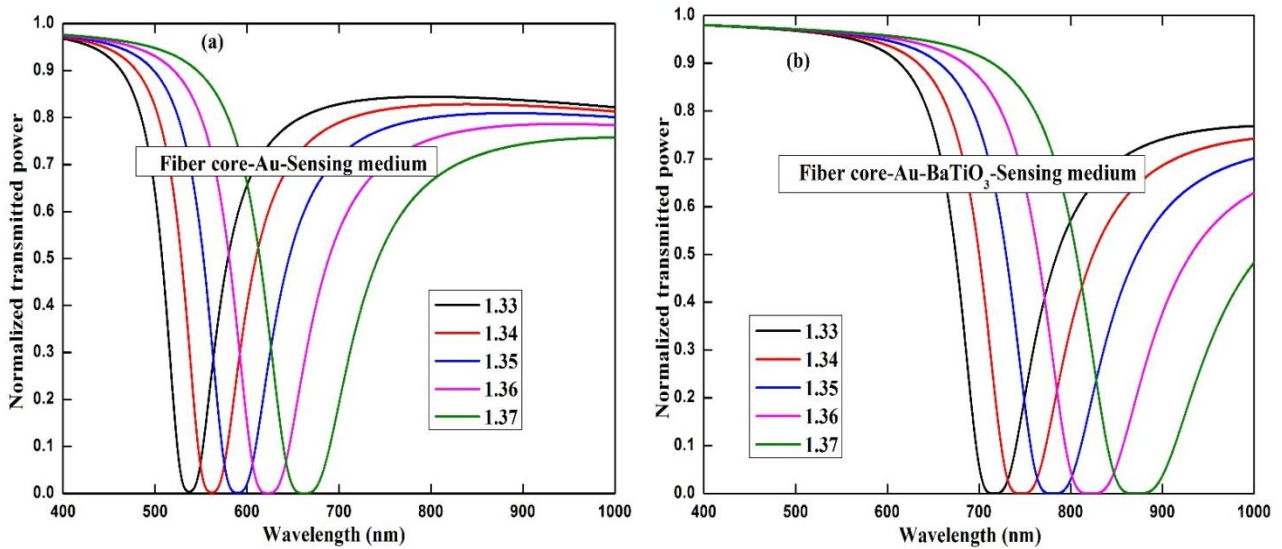


Fig. 4. Transmission spectra plot of Au based fiber SPR sensor (a) without BaTiO₃ layer (b) with BaTiO₃ layer (color online)

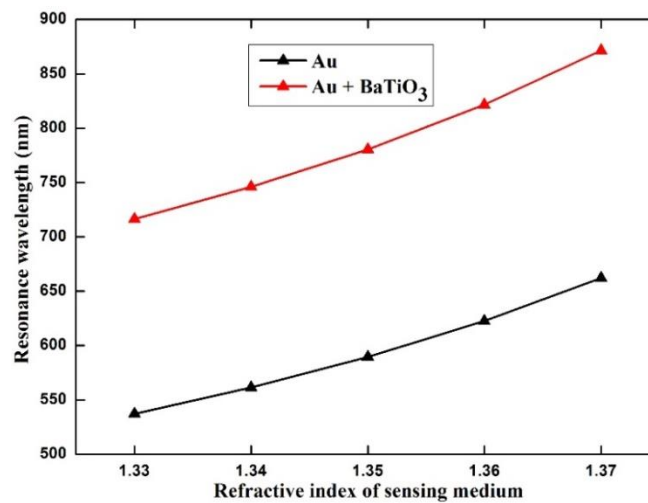


Fig. 5. Plot of resonance wavelength (nm) variation with various refractive indexes for Au-based fiber SPR sensor with and without BaTiO₃ layer (color online)

In the second configuration, we have considered the Au metal layer with the BaTiO₃ layer for RI ranging from 1.33 to 1.37. Fig. 4 (a) depicts the normalized transmitted power spectra for the Au based fiber SPR sensor without the BaTiO₃ layer. In this plot, the resonance wavelength is obtained at 537.1 nm for the RI of 1.33. The shift in resonance wavelength from 537.1 nm to 716.4 nm is obtained with the addition of the BaTiO₃ layer as illustrated in Fig. 4(b). The resonance wavelengths for the

Ag-based fiber SPR sensor are obtained at 561.4 nm, 589.5 nm, 622.5 nm, and 662.1 nm for the RI of 1.34, 1.35, 1.36, and 1.37 respectively. Similarly, the resonance wavelengths for the Au+BaTiO₃ based fiber SPR sensor are obtained at 746 nm, 780.5 nm, 821.6 nm, and 871.6 nm for the RI of 1.34, 1.35, 1.36, and 1.37 respectively. Fig. 5 depicts the resonance wavelength variation with the various RI with and without the BaTiO₃ layer for the Au based fiber SPR sensor.

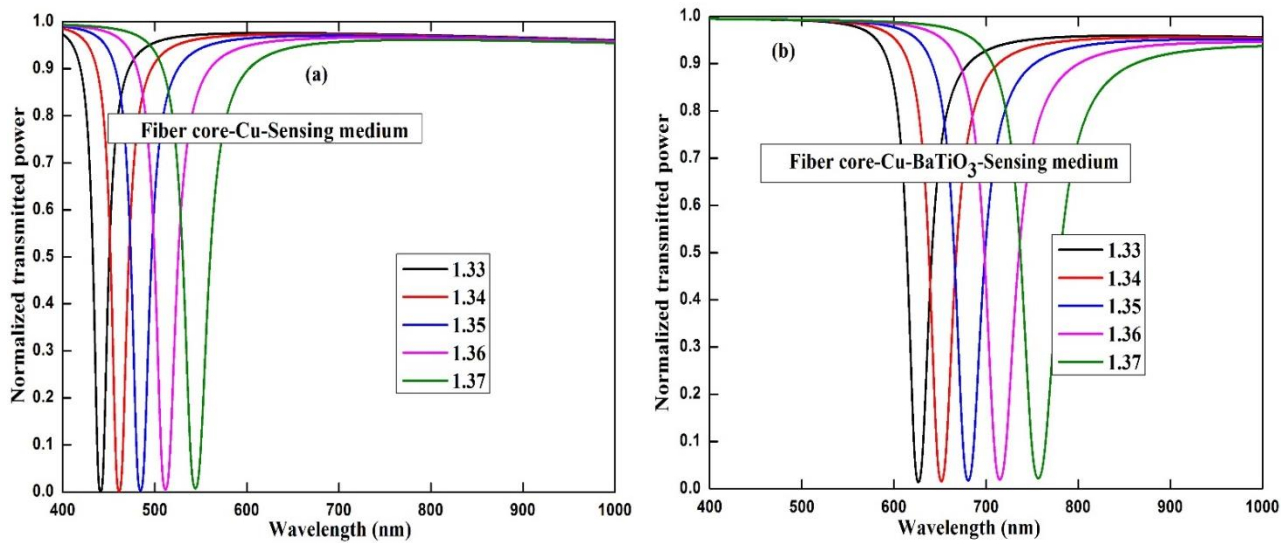


Fig. 6. Transmission spectra plot of Cu based fiber SPR sensor (a) without BaTiO₃ layer (b) with BaTiO₃ layer (color online)

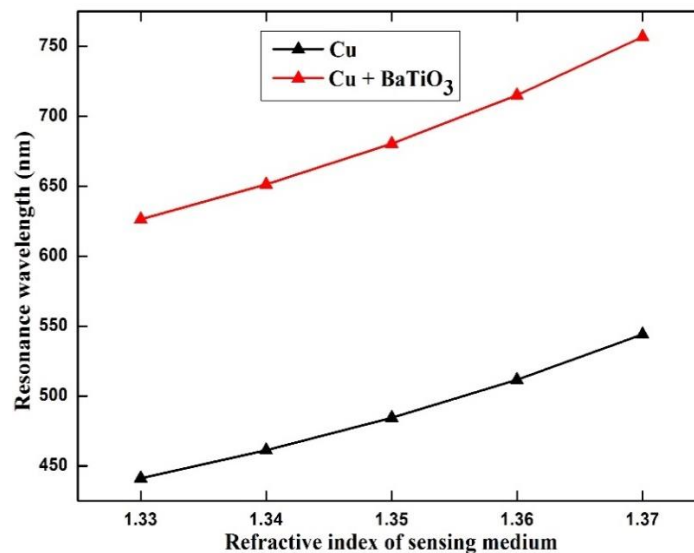


Fig. 7. Plot of resonance wavelength (nm) variation with various refractive indexes for Cu-based fiber SPR sensor with and without BaTiO₃ layer (color online)

Table 1. Sensitivity of the proposed structure with different configurations

Refractive index of sensing medium/ Structure configuration	Sensitivity (nm/RIU)					
	Core/Cu /sensing medium	Core/Cu /BaTiO ₃ / sensing medium	Core/Ag /sensing medium	Core/Ag /BaTiO ₃ / sensing medium	Core/Au /sensing medium	Core/Au /BaTiO ₃ / sensing medium
1.34	2010	2500	2140	2630	2430	2960
1.35	2165	2705	2305	2855	2620	3205
1.36	2350	2954	2500	3117	2847	3507
1.37	2575	3257	2740	3442	3125	3880

Table 2. Comparison of proposed structure with other existing fiber based SPR structure

S. No.	Structure	Refractive index of the sensing medium	Highest Sensitivity (nm/RIU)	Reference
1.	Core/Au/BaTiO ₃ /sensing medium	1.33-1.37	3880 nm/RIU	This work
	Core/Ag/BaTiO ₃ /sensing medium	1.33-1.37	3442 nm/RIU	
	Core/Cu/BaTiO ₃ /sensing medium	1.33-1.37	3257 nm/RIU	
2.	Core/Ag/Au/MoS ₂ /sensing meidum	1.33-1.37	3061 nm/RIU	[40]
3.	Core/ITO/ZnO/sensing meidum	1.33-1.37	1620 nm/RIU	[41]

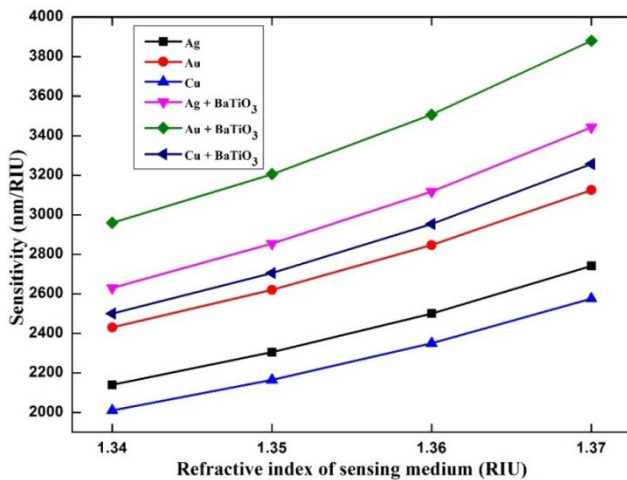


Fig. 8. Plot of sensitivity (nm/RIU) with various refractive indexes for different configuration of fiber SPR sensor (color online)

In the third configuration, the Cu metal layer with the BaTiO₃ layer is considered for the RI ranging from 1.33 to 1.37. Here, resonance wavelength is obtained at 441.1 nm for the RI of 1.33 without the BaTiO₃ layer as depicted in Fig. 6 (a). The resonance wavelength shifts to 626.4 nm with the addition of the BaTiO₃ layer as illustrated in Fig.

6 (b). The resonance wavelengths for the Cu based fiber SPR sensor are obtained at 461.2 nm, 484.4 nm, 511.6 nm, and 544.1 nm for the RI of 1.34, 1.35, 1.36, and 1.37 respectively, and with the inclusion of BaTiO₃ layer, these shift to 651.4 nm, 680.5 nm, 715 nm and 756.7 nm in the Cu+BaTiO₃ based fiber SPR sensor. The resonance wavelength variation with the various RI with and without the BaTiO₃ layer in the Cu based fiber SPR sensor is represented in Fig. 7. These three configurations with their respective sensitivity are given in Table 1 and are plotted in Fig. 8. Finally, we have shown the comparison of this work with the existing similar works in Table 2. It is concluded that the highest sensitivity of 3880 nm/RIU is attained with the Au + BaTiO₃ based fiber SPR sensor for the RI ranging from 1.33 to 1.37. Hence the proposed structure can be suitable in biosensing applications.

4. Conclusion

In this work, we have studied the fiber SPR sensor with three different metal layers and the spectral responses of this multilayer structure have been analyzed using numerical simulation. We have shown the comparative outcomes among the three metals (Ag/Au/Cu) and obtained better sensitivity of 3125 nm/RIU with the gold layer. To improve the sensor performance, we include a

protective layer of BaTiO₃ that enhances the sensitivity. Here maximum sensitivity of 3880 nm/RIU is attained with the Au-BaTiO₃ based fiber SPR sensor. In conclusion, the addition of the Barium Titanate layer improves sensor performance in terms of sensitivity. Therefore, this study is expected to offer a highly sensitive SPR biosensor with its promising potential applications in biological and chemical fields.

Acknowledgments

The authors are thankful the ECE Department, Malaviya National Institute of Technology, India, for all the help required to carry out this study.

References

- [1] P. Bhatia, P. Yadav, B. D. Gupta, *Sensors Actuators B* **182**, 330 (2013).
- [2] K. B. Min, S. J. Yoon, D. Kim, *Appl. Opt.* **47**(31), 5886 (2008).
- [3] N. Mudgal, A. Saharia, A. Agarwal, J. Ali, P. Yupapin, G. Singh, *Opt. Quant. Electron.* **52**, 307 (2020).
- [4] E. Kretschmann, H. Raether, *Zeitschrift für Naturforschung A* **23**(12), 2135 (1968).
- [5] J. Homola, M. Piliarik, "Surface Plasmon Resonance Based Sensors", fourth ed., Springer, 2006.
- [6] Y. Vasimalla, H. S. Pradhan, R. J. Pandya, *Appl. Opt.* **59**(24), 7299 (2020).
- [7] N. Mudgal, M. K. Falaswal, T. Ismail, I. S. Fahim, M. Tiwari, G. Singh, *Optical and Wireless Technologies, Lecture Notes in Electrical Engineering* **648**, 353 (2020).
- [8] J. A. Kim, T. Hwang, S. R. Dugasani, R. Amin, A. Kulkarni, S. H. Park, T. Kim, *Sens. Actuators B* **187**, 426 (2013).
- [9] A. K. Mishra, S. K. Mishra, B. D. Gupta, *Opt. Commun.* **344**, 86 (2015).
- [10] R. C. Jorgenson, S. S. Yee, *Sens. Actuators B* **12**(3), 213 (1993).
- [11] B. Kaur, S. Kumar, B. K. Kaushik, *IEEE Sensors Journal* **21**(21), 23957 (2021).
- [12] V. S. Chaudhary, D. Kumar, S. Kumar, *IEEE Sensors Journal* **21**(16), 17800 (2021).
- [13] A. Verma, A. Prakash, R. Tripathi, *Opt. Commun.* **357**, 106 (2015).
- [14] C. Yue, Y. Lang, X. Zhou, Q. Liu, *Appl. Opt.* **58**(34), 9411 (2019).
- [15] L. Xia, S. Yin, H. Gao, Q. Deng, C. Du, *Plasmonics* **6**(2), 245 (2011).
- [16] Y. Feng, Y. Liu, J. Teng, *Appl. Opt.* **57**(14), 3639 (2018).
- [17] B. Liedberg, C. Nylander, M. I. Ljunstro, *Sens. Actuators* **4**, 299 (1983).
- [18] S. Kaushik, U. K. Tiwari, S. S. Pal, R. K. Sinha, *Biosens. Bioelectron.* **126**, 501 (2019).
- [19] H. Yan, D. Han, M. Li, B. Lin, *J. Nanophotonics* **11**, 016008 (2017).
- [20] N. Mudgal, A. Saharia, A. Agarwal, G. Singh, *IETE Journal of Research* (2020).
DOI: 10.1080/03772063.2020.1844074
- [21] R. K. Gangwar, R. Min, S. Kumar, X. Li, *Front. Phys.* **9**, (2021).
- [22] B. Kaur, S. Kumar, B. K. Kaushik, *Biosens. Bioelectron.* **197**, 113805 (2022).
- [23] L. Wang, W. Zhu, W. Lu, X. Qin, X. Xu, *Biosens. Bioelectron.* **111**, 41 (2018).
- [24] N. F. Chiu, Y. C. Tu, T. Y. Huang, *Sensors* **14**(1), 170 (2014).
- [25] H. Wang, H. Zhang, J. Dong, S. Hu, W. Zhu, W. Qiu, H. Lu, J. Yu, H. Guan, S. Gao, Z. Li, W. Liu, M. He, J. Zhang, Z. Chen, Y. Luo, *Photonics Res.* **6**(06), 485 (2018).
- [26] S. W. Zeng, S. Y. Hu, J. Xia, T. Anderson, X. Q. Dinh, X. M. Meng, P. Coquet, K. T. Yong, *Sensor, Actuat. B-Chem.* **207**, 801 (2015).
- [27] Y. Singh, S. K. Raghuvanshi, *IEEE Sensors Letters* **3**(12), 3502704 (2019).
- [28] Y. Wang, J. Dong, Y. Luo, J. Tang, H. Lu, J. Yu, H. Guan, J. Zhang, Z. Chen, *IEEE Photonics Journal* **9**(6), 4801309 (2017).
- [29] N. Mudgal, P. Yupapin, J. Ali, G. Singh, *Plasmonics* **15**, 1221 (2020).
- [30] L. Liu, M. Wang, L. Jiao, T. Wu, F. Xia, M. Liu, W. Kong, L. Dong, M. Yun, *J. Opt. Soc. Am. B* **36**(4), 1108 (2019).
- [31] A. Yadav, S. Sudhanva, P. Sharan, A. Kumar, *Int. J. Inf. Technol.* **13**, 2163 (2021).
- [32] S. Fouad, N. Sabri, Z.A.Z. Jamal, P. Poopalan, *J. Nano- Electron. Phys.* **8**(2), 04085 (2016).
- [33] R. K. Verma, B. D. Gupta, *J. Opt. Soc. Am. A* **27**(4), 846 (2010).
- [34] M. A. Ordal, L. L. Long, R. J. Bell, S. E. Bell, R. R. Bell, R. W. Alexander, C. A. Ward, *Appl. Opt.* **22**(7), 1099 (1983).
- [35] S. H. Wemple, J. M. Didomenico, I. Camlibel, *J. Phys. Chem. Solids* **29**, 1797 (1968).
- [36] M. Yamamoto, *Tutor Rev. Polarogr.* **48**, 209 (2002).
- [37] A. Sharma, B. D. Gupta, *Photon. Nanostruct.- Fundam. Appl.* **3**, 30 (2005).
- [38] S. Gan, Y. Zhao, X. Dai, Y. Xiang, *Results in Physics* **13**, 102320 (2019).
- [39] L. Wu, J. Guo, Q. Wang, S. Lu, X. Dai, Y. Xiang, D. Fan, *Sens. Actuat. B Chem.* **249**, 542 (2017).
- [40] Q. Wang, X. Jiang, L-Y Niu, X-C Fan, *Optics and Lasers in Engineering* **128**, 105997 (2020).
- [41] V. Kapoor, N. K. Sharma, V. Sajal, *Optik* **185**, 464 (2019).